water

MDPI

Article

Working Mode Identification Method for High Arch Dam Discharge Structure Based on Improved Wavelet Threshold–EMD and RDT Algorithm

Yingjia Guo [1,2], Zongzhe You [1] and Bowen Wei [1,*]

[1] School of Infrastructure Engineering, Nanchang University, Nanchang 330031, China
[2] College of Water Conservancy and Ecological Engineering, Nanchang Institute of Technology, Nanchang 330099, China
* Correspondence: bwwei@ncu.edu.cn

Abstract: Prototype vibration response data of high arch dam discharge structures inevitably mix various noises under the discharge excitation, which adversely affects the accuracy of the working modal identification of the structure. To effectively filter noise and reduce modal aliasing for better identification accuracy, this study proposes an improved modal threshold identification method based on an improved wavelet threshold–empirical mode decomposition (EMD) and random decrement technique (RDT) algorithm for high arch dam discharge structures. On the basis of the measured vibration response data of the dam, the wavelet threshold is adopted to filter out most of the high-frequency white noise and to reduce the boundary accumulation effect of EMD decomposition. Detrended fluctuation analysis (DFA) is utilized to filter white noise and low-frequency flow noise after EMD decomposition. The natural frequency and damping ratio of the structure system are obtained by the improved RDT algorithm. The engineering examples show that the proposed method can accurately filter the measured vibration response signal noise of the discharge structure, retain the signal characteristic information, improve the accuracy of working modal recognition of the structural vibration response, avoid the complex ordering process of the system, and ease the working modal parameter identification of high arch dam discharge structures. This method can be applied to the mode identification of other large structures, as well.

Keywords: high arch dam; signal processing; working modal identification; vibration under discharge excitation; noise reduction

Citation: Guo, Y.; You, Z.; Wei, B. Working Mode Identification Method for High Arch Dam Discharge Structure Based on Improved Wavelet Threshold–EMD and RDT Algorithm. *Water* **2022**, *14*, 3735. https://doi.org/10.3390/w14223735

Academic Editors: Jie Yang, Lin Cheng, Chunhui Ma and Giuseppe Pezzinga

Received: 13 September 2022
Accepted: 15 November 2022
Published: 17 November 2022

1. Introduction

High arch dams are located in deep mountain valleys, which have a large flow per unit width and high flood peak energy during discharging. Flood-induced vibrations of arch dams are a key technical problem related to the safety of arch dam structures. Modal parameter identification of discharge structures is an important technical approach to confirm the operating state of dam structures [1–8]. Various monitoring facilities have been applied to monitor the environmental variables and vibration responses of dams. Noises are inevitably contained in the prototype vibration response data of discharge structures due to the complex working environment of data collection and the difficulty in excitation of large discharge structures. The condition considerably affects the accuracy of working modal identification of discharge structures. Therefore, it is necessary to eliminate the environmental background noise and to accurately identify the modal parameters of the high arch dam discharge structure under the working environment load excitation.

Based on the identification of structural modal parameters under environmental excitation, traditional modal identification methods, including stochastic subspace identification (SSI) [9,10], RDT [11], Hilbert–Huang Transform (HHT) [12,13], etc., have been successfully

applied in the identification of structural modal parameters under environmental excitation. The frequency domain decomposition method was applied by Li [14,15] to identify the modal parameters of a high arch dam under discharge excitation, which verified the feasibility of identifying the working modal parameters of the structure by using only the fluid-induced vibration response of the structure. Tian et al. [16,17] applied RDT to the working modal identification of a cantilever beam. However, RDT seems to be powerless for dealing with non-stationary signals. Zhang et al. [18] applied the HHT method to identify the modal parameters of the dam discharge structure. The ability of HHT to identify the frequency-intensive structure is confirmed, but there are end effects, modal aliasing, and other defects in the actual calculation process. Therefore, the method of combining RDT with HHT to suppress the deficiencies of the two methods has been proposed by many experts. He et al. [19,20] combined HHT and RDT to identify the working mode of the Nanjing Yangtze River Bridge. Han et al. [21] applied HHT–RDT method to the working mode identification of structures under seismic action. However, the original signal obtained by the prototype vibration response test under the discharge excitation had a certain deviation due to the existence of background noise. Accordingly, an accurate reflection of the mechanical characteristics of the structure could not be obtained. Noise reduction of the prototype vibration response data is essential to obtain accurate structural feature information. For the noise reduction of signals, many experts have conducted a series of discussions. Tang et al. [22–24] applied wavelet analysis for signal denoising, but the filtering effect mainly depends on the selection of the wavelet threshold. Zhao et al. [25,26] applied the EMD method for signal decomposition based on the time-scale characteristics of the data. It is easy for the mixed noise and white noise signals to cause a loss of effective information. Li et al. [27,28] applied the wavelet threshold denoising method based on EMD. However, EMD decomposition leads to different degrees of end effects and modal aliasing when the signal contains sound noise or white noise [29]. Zhang et al. [30,31] applied the hybrid method of wavelet analysis and EMD noise reduction, which can effectively extract the value information of low-SNR discharge structures, but the wavelet basis is difficult to determine.

On the basis of the above-mentioned studies on theoretical analysis and simulation experiments of high arch dam discharge structure, this study proposes an improved wavelet threshold–EMD and RDT algorithm for working modal identification of high arch dams. Prior to modal identification, the improved wavelet threshold–EMD algorithm is used to effectively process the signal. The improved wavelet threshold function is used to filter out most of the high-frequency white noise and reduce the boundary accumulation effect of EMD decomposition. The white noise and low-frequency flow noise are further filtered by DFA after EMD decomposition. The improved RDT algorithm is applied to the working mode identification of the high arch dam discharge structure. The EMD process of the vibration response signal is controlled by a band-pass filter to obtain each modal component of the structure, the free attenuation signal of each modal component is extracted by RDT method, and the natural frequency and damping ratio of the high arch dam discharge structure are obtained by HHT and least squares fitting. The method is applied to the measured vibration response analysis of a high arch dam structure.

2. Basic Theory

2.1. Improved Wavelet Threshold–EMD Hybrid Algorithm for High Arch Dam Noise Reduction

The data collection working environment of the high arch dam discharge structure is complicated, and the vibration interference type is shown in Figure 1. Some low-frequency interference signals and white noise are mixed in the prototype vibration response data of the discharge structure. An improved wavelet threshold–EMD hybrid algorithm is proposed to filter noise in the discharge structure response of arch dams in order to retain a large number of useful signals in the original signal.

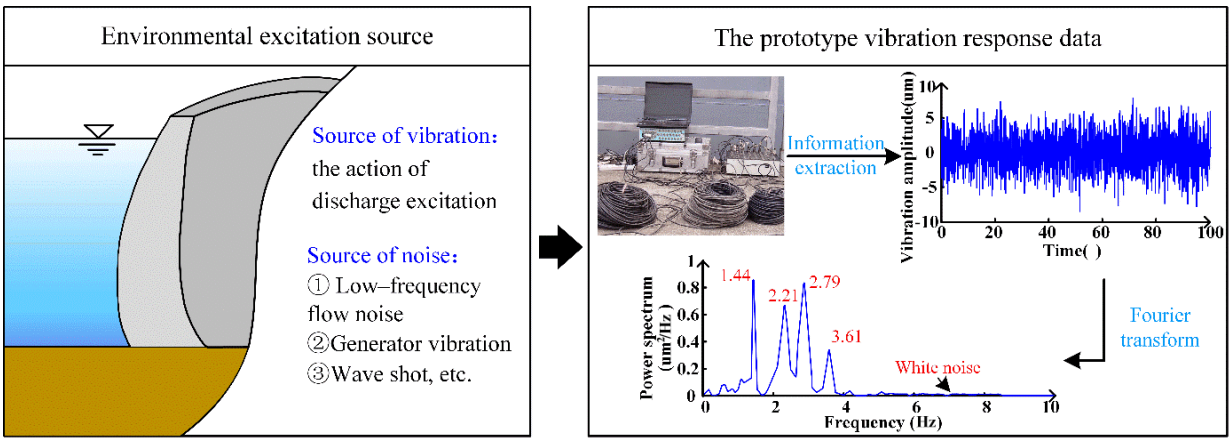

Figure 1. Prototype vibration response of the arch dam.

This method fully combines the advantages of wavelet threshold and EMD denoising: wavelet threshold is used to separate the high-frequency noise in the signal, to suppress the endpoint effect of EMD, to reduce the influence of mode mixing, and to lay a foundation for the subsequent EMD noise reduction; EMD decomposition further separates the white noise and low-frequency flow noise and improves noise reduction accuracy. The basic principle is as follows:

The key to wavelet threshold denoising [32,33] is not only the selection of the threshold function, but also the estimation of the wavelet threshold size. The main idea of signal denoising is to reconstruct the compressed coefficient on the basis of the preset wavelet transform coefficient of the compressed signal.

In selecting the wavelet threshold, the threshold selection method of traditional wavelet threshold denoising is:

$$\mathrm{T} = \sigma_n \sqrt{2 \ln N} \tag{1}$$

where σ_n is the standard deviation and N is the signal length.

For the vibration signal of the discharge structure submerged by noise, the wavelet coefficient of the noise decreases with the increase of the number of decomposition layers, which affects the noise reduction effect. The traditional threshold formula calculates the global threshold, which is obviously not suitable for the noise reduction processing in this study. An improved wavelet threshold denoising method is proposed. The number of decomposition layers j is determined by a white noise test [34]. The threshold functions of each layer are designed according to the number of decomposition layers j. The noise components in the high-frequency coefficients are separated to completely eliminate the noise components while retaining the original useful signal. The improvement process is expressed as:

$$T = t\sigma e^{\sigma} N_j \sqrt{2 \lg N_j} / \lg(j+1) \tag{2}$$

where N_j is the signal data length; j is the number of decomposition layers; and σ is the standard variance of noise, whose calculation formula can be written as:

$$\sigma = median(abs(D))/0.5 * N_j) \tag{3}$$

where D is the absolute median of the high-frequency coefficient.

Traditional threshold functions include the soft threshold function and the hard threshold function. The hard threshold function is used to keep the wavelet coefficient constant

when the absolute value of the wavelet coefficient is greater than or equal to the given threshold value, otherwise it should be set to zero. The formula is as follows:

$$\hat{w}_{j,k} = \begin{cases} w_{j,k}, & \left|w_{j,k}\right| \geq T \\ 0, & \left|w_{j,k}\right| < T \end{cases} \tag{4}$$

where $\hat{w}_{j,k}$ is the estimated wavelet coefficient after the threshold is applied, and $w_{j,k}$ is the wavelet decomposition coefficient of the signal.

The soft threshold function is used to subtract the threshold when the absolute value of the wavelet coefficient is greater than or equal to a given threshold, otherwise it should be set to zero. The formula is as follows:

$$\hat{w}_{j,k} = \begin{cases} \mathrm{sgn}(w_{j,k})(\left|w_{j,k}\right| - T) & \left|w_{j,k}\right| \geq T \\ 0, & \left|w_{j,k}\right| < T \end{cases} \tag{5}$$

The hard threshold function can effectively preserve local features such as signal edges. The soft threshold algorithm is relatively smooth but will cause distortion phenomena such as edge blur. To overcome the shortcomings of the soft and hard threshold algorithms, this study proposes an improved wavelet threshold function, which is defined as follows:

$$\hat{w}_{j,k} = \begin{cases} \mathrm{sgn}(w_{j,k})[\left|w_{j,k}\right| - tTe^{(1-t)(T-|w_{j,k}|)}] & \left|w_{j,k}\right| \geq T \\ 0 & \left|w_{j,k}\right| < T \end{cases} \tag{6}$$

where t is the adjustment factor.

When $\left|w_{j,k}\right| \geq T$, the following function can be obtained as:

$$f(x) = \mathrm{sgn}(x)[|x| - tTe^{(1-t)(T-|x|)}] \tag{7}$$

Thus,

$$\begin{cases} \frac{f(x)}{x} = \frac{[x - tTe^{(1-t)(T-x)}]}{x} = 1 - \frac{tTe^{(1-t)(T-x)}}{x} \to 1 (x \to +\infty) & x > 0 \\ \frac{f(x)}{x} = \frac{[x + tTe^{(1-t)(T+x)}]}{x} = 1 + \frac{tTe^{(1-t)(T+x)}}{x} \to 1 (x \to -\infty) & x < 0 \end{cases} \tag{8}$$

The improved threshold function is equivalent to a function between the soft and hard threshold functions. When the original signal contains a large number of sharp mutations, T is moved toward the hard threshold direction. On the contrary, when the original signal is relatively smooth, T is moved toward the soft threshold. Thus, the size of T can be adjusted adaptively to obtain an excellent denoising effect.

The improved wavelet threshold noise reduction filters out high-frequency white noise in the signal while reducing EMD endpoint effects and modal aliasing. The EMD noise reduction is further performed on the vibration signal, and the white noise and the low-frequency water flow noise are further filtered.

The EMD method [35,36] iteratively decomposes several IMF components and one residual signal by using the screening process based on the cubic spline interpolation method for the signal $x(t)$, which can be expressed as:

$$x(t) = \sum_{j=1}^{n} c_j(t) + r_n(t) \tag{9}$$

where n is the number of decomposed IMF components and $r_n(t)$ is the residual signal of $x(t)$.

The iterative screening of IMF components [37] is an important part of EMD decomposition. According to the orthogonality of EMD decomposition, if the decomposition is correct, the IMF components are orthogonal to each other, and the IMF orthogonal index is defined as:

$$IO = \sum_{t=0}^{T} \left(\sum_{i=1}^{n+1} \sum_{j=1}^{n+1} IMF_i(t) \times IMF_j(t) / x(t)^2 \right) \tag{10}$$

If the orthogonal index is small, the modal components are uncorrelated and no modal aliasing occurs; conversely, the modal aliasing is severe. Traditional threshold parameters are replaced by the orthogonal index to control the IMF screening process and to increase the frequency-intensive structure-identification ability of EMD decomposition. The orthogonal index *IO* reaches the minimum by the number of iterations of different IMF and is expressed as:

$$x(N) = \text{argmin}(IO) \tag{11}$$

where N is the number of iterations per level IMF.

DFA [38,39] is adopted to determine the EMD threshold of the remaining IMF components to further filter out the noise. The formula for calculating the index α_i is shown as follows:

$$\alpha_i = \frac{\log_2 F(s)}{\log_2 s} = \frac{\log_2 [\frac{1}{2N_S} \sum_{v=1}^{2N_s} F^2(v,s)]}{2 \log_2 s} \tag{12}$$

Theoretically, the corresponding sequences are white noise, pink noise, and brown noise when $\alpha_i \leq 0.5$, $0.5 < \alpha_i < 1$, and $1 \leq \alpha_i < 1.5$, respectively. The noise of vibration response data of the discharge structure is mostly white noise. In this paper, only the white noise is considered, and the threshold for white noise is taken as $0 < \alpha_i < 0.5$. In addition, the noise in the prototype vibration signal of the arch dam is filtered with the improved wavelet threshold and EMD algorithm.

2.2. Modal Parameter Identification of High Arch Dam Discharge Structures Based on Improved HHT–RDT Algorithm

A modal identification method based on the HHT–RDT algorithm is proposed for the measured vibration response data of high arch dam structures in this paper. The HHT method is used to extract the modal response components of each order, and the RDT method is used to extract the feature information of each order component, so as to make up for the shortcomings of the two methods.

RDT is a processing method for extracting the free vibration response from the random response signal of structures. The method uses the property of the vibration signal mean value in the stationary stochastic process to identify the deterministic or random vibration signals and then extract the deterministic vibration signal.

For the linear system, assuming that $X_1(t)$ and $X_2(t)$ are the structural response data satisfying the gaussian distribution, according to the trigger condition, their random decrement cross-correlation function is:

$$C_{x_i}(t_i) = [c_1 \leq X_i(t_i) \leq c_2] \tag{13}$$

$$D_{x_2x_1}(\tau) = E[X_1(t_i + \tau) | C_{x_1}(t_i)] \tag{14}$$

$$D_{x_2x_1}(\tau) = E[X_2(t_i + \tau) | C_{x_1}(t_i)] \tag{15}$$

where $E[\cdot]$ represents the mathematical expectation of the cross-correlation function, which can be written as:

$$D_{x_1x_1}(\tau) = \frac{R_{x_1x_1}(\tau)}{\sigma^2{}_{x_1}} \overline{a} - \frac{R_{x_1x_1}(\tau)}{\sigma^2{}_{\dot{x}_1}} \overline{b} \tag{16}$$

$$D_{x_2x_1}(\tau) = \frac{R_{x_2x_1}(\tau)}{\sigma^2{}_{x_1}} \overline{a} - \frac{R_{x_2x_1}(\tau)}{\sigma^2{}_{\dot{x}_1}} \overline{b} \tag{17}$$

$$D_{x_2x_1}(\tau) = E[X_2(t_i + \tau)|C_{x_1}(t_i)] \tag{18}$$

where $R_{x_ix_1}(\tau) = E[X_i(t)X_1(t+\tau)], (i = 1, 2), \overline{a} = \frac{\int_{\alpha}^{\alpha_2} x p_{x_1}(x)dx}{\int_{\alpha}^{\alpha_2} p_{x_1}(x)dx}, \overline{b} = \frac{\int_{b}^{b_2} \dot{x} p_{\dot{x}_1}(\dot{x})d\dot{x}}{\int_{b}^{b_2} p_{\dot{x}_1}(\dot{x})d\dot{x}}$.

For complex structures such as high arch dams, the structure composition is not a single linear system, but a multi-degree-of-freedom system. Therefore, the motion equation of arch dam structures under environmental excitation can be written as:

$$M\ddot{X}(t) + C\dot{X}(t) + KX(t) = F(t) \tag{19}$$

where M, C, and K are the mass matrix, damping matrix, and stiffness matrix of the arch dam structure, respectively; x is the displacement vector; and $F(t)$ is the external excitation load vector.

Assuming that the external force is a stationary Gaussian stochastic process with a mean of zero, in the case where the mass, damping, and stiffness matrices are determined, R_{xx_k} is the homogeneous solution of the equation of motion and is shown as:

$$M\ddot{R}_{xx_k}(\tau) + C\dot{R}_{xx_k}(\tau) + KR_{xx_k}(\tau) = 0 \tag{20}$$

The RDT function can be estimated as:

$$\hat{R}_{x_jx_k}(\tau) = \frac{1}{n}\sum_{i=1}^{N} x_j(t_i + \tau)\Big|C_{x_k(t_i)} \tag{21}$$

where $\hat{R}_{x_jx_k}(\tau)$ is the random decrement function of $X_j(t)$ for $X_k(t)$; N is the total number of trigger events; $C_{x_1}(t_i)$ is the specified punctual trigger condition; and t_i is the ith moment.

In this paper, the waveform components of each order are obtained by the HHT method before identification by the RDT method. According to the approximate range of the main frequency reflected by the self-power spectrum of the signal, the pre-nth order natural frequency distribution of the system is obtained ($w_{1L} < w_1 < w_{1R}$, $w_{2L} < w_2 < w_{2R}$, $\cdots$, $w_{nL} < w_n < w_{nR}$). If the i-th modal response component is solved, the input signal $X_j(t)$ is passed through a filter having a bandpass frequency of $w_{iL} < w_i < w_{iR}$. After obtaining n waveform components, EMD is performed on each waveform component, and the obtained first-order natural mode function is used as a modal component. The modal response components obtained are stationary signals. The free-decay response function of each modal component is extracted by the RDT algorithm, which can be expressed as:

$$x(t) = e^{-\xi w_0 t}(x_0 \cos(\omega_d t) + \frac{x_0 + \xi\omega_0 x_0}{\omega_d} \sin(\omega_d t)) \tag{22}$$

where ω_0 is the natural frequency of the system; ξ is the relative damping coefficient; x_0 and $\dot{x}_0$ are the initial displacement and velocity, respectively; and $\omega_{\mathrm{d}} = \omega_0\sqrt{1-\xi^2}$ is the damped natural frequency.

In addition, the expression can also be written as:

$$x(t) = A_0 e^{-\xi w_0 t}(x_0 \cos(\omega_d t) + \varphi_0) \tag{23}$$

where A_0 is a constant, which is related to the excitation load intensity, structure mass, and frequency characteristics. HT is applied to obtain the analytical signal of *x(t)* as:

$$z(t) = x(t) + jH(x(t)) = A(t)e^{-j\theta(t)} \tag{24}$$

When the damping in the system is small, the amplitude and phase in the equation can be expressed as:

$$A(t) = A_0 e^{-\xi\omega_0 t}, \quad \theta(t) = \omega_d t + \varphi_0 \tag{25}$$

The amplitude and phase functions of the equation above are analyzed by logarithmic and differential operators, respectively, to obtain:

$$\ln A(t) = -\xi\omega_0 t + \ln A_0, \quad \omega(t) = \frac{d\theta(t)}{dt} = \omega_d \tag{26}$$

The natural frequency ω_0 and damping ratio of the system can be obtained by $\omega_d = \omega_0\sqrt{1-\xi^2}$. Therefore, the natural frequency and damping ratio of the structure are obtained.

2.3. Recognition Process Based on Improved Wavelet Threshold–EMD and RDT Algorithm

Based on the above-mentioned theories, the construction procedure of modal parameter identification of high arch dam discharge structures based on improved wavelet threshold–EMD and RDT algorithm is shown in Figure 2.

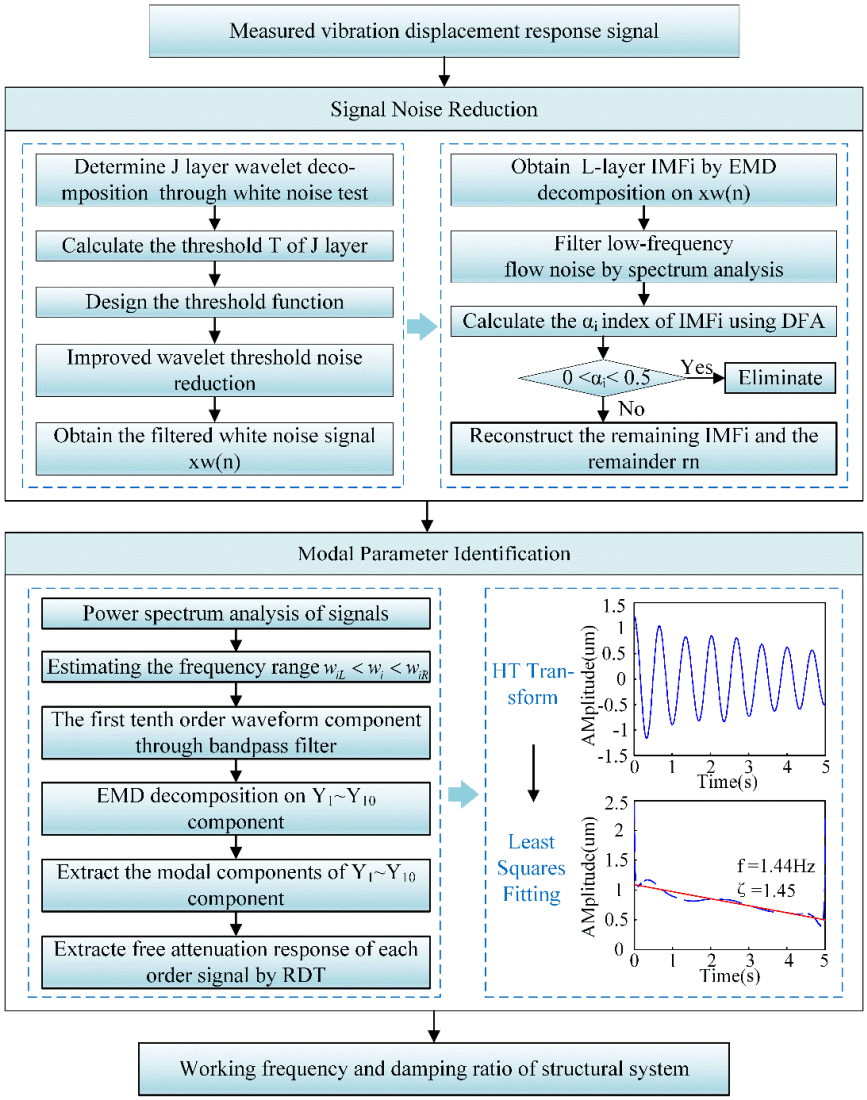

Figure 2. Flow chart of modal parameter identification of high arch dam discharge structures.

3. Application Case

3.1. Engineering Data

The barrage is a typical high arch dam with a dam crest elevation of 1205 m and a maximum height of 240 m. To accurately obtain the working behavior of the arch dam, the measured points were arranged at the dam crest arch and the arch crown beam. Among

them, the arch ring was arranged with seven horizontal dynamic displacement measuring points B1–B7 from the left bank to the right bank, and the crown beam was arranged with four horizontal dynamic displacement measuring points B8–B11 from the top to the bottom of the dam. The arrangement of arch dam prototype flood discharge vibration measurement points is shown in Figure 3, and the test conditions of the discharge vibration of the arch dam prototype are shown in Table 1. The dynamic displacement sensor was a DP seismic low-frequency displacement sensor with a frequency response range of 0.35–200 Hz and a sensitivity of 8–15 mv/μm. The DASP data acquisition and processing system was used for data acquisition. The sampling frequency was 200 Hz, the sampling time was 300 s, and the collected data points totaled 6000. The new method was demonstrated using the sampling data of the displacement monitoring data of the arch dam.

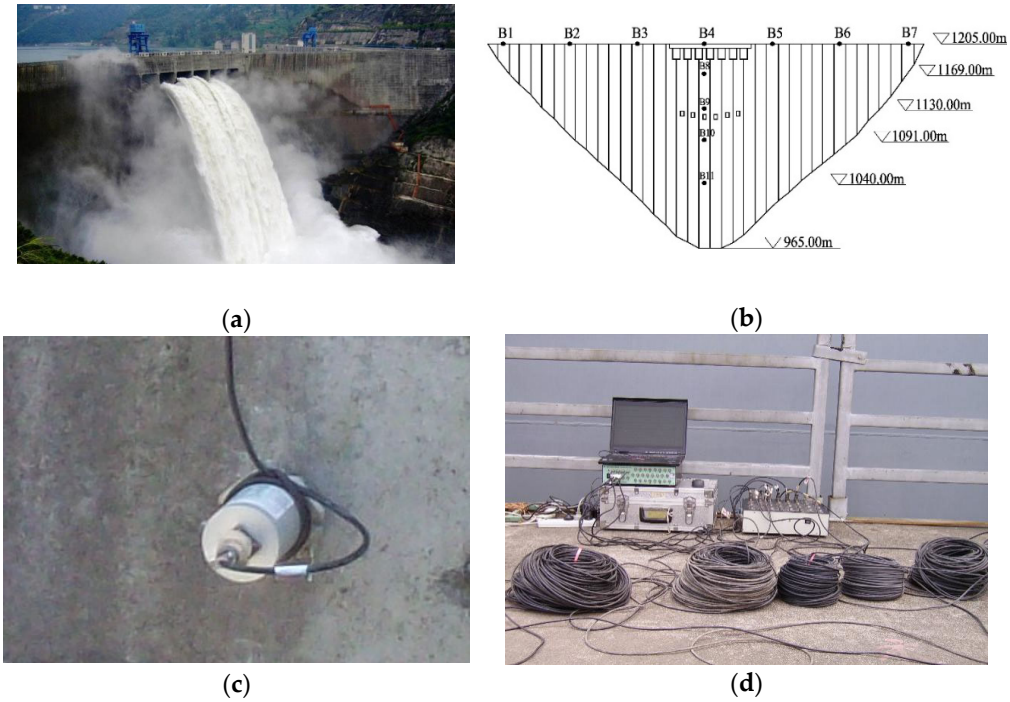

Figure 3. Arrangement of arch dam prototype flood discharge vibration measurement points. (**a**) The arch dam prototype; (**b**) Sensor arrangement for the arch dam vibration test; (**c**) DP-type dynamic displacement sensor; (**d**) DASP signal acquisition system.

Table 1. Test conditions of discharge vibration of arch dam prototype.

Condition	Spillway Opening	Upstream Water Level (m)	Downstream Water Level (m)
1	Fourth surface spillway and first tunnel spillway	1196.00	1014.36
2	Third, fourth surface spillway and first tunnel spillway	1196.01	1014.50

In the process of signal acquisition, the vibration response data of the discharge structure of the arch dam under discharge excitation easily mixed with some noises that covered up the useful signals, which will affect the accuracy of vibration response analysis of the test results. The time history signals and power spectra of typical B2, B3, B4, and B8 measuring points under working condition 2 are shown in Figures 4–7. For the measured points B2 and B3 at the arch ring, the measuring points of the dam body near the dam shoulder had more vibration frequency components, and the vibration amplitude was smaller as it was closer to the dam shoulder. For the measuring points B4 and B8 of the arch crown beam, the vibration energy of the dam body of the high-frequency component was less than that of the low-frequency component, and the high-frequency peak was

submerged by the low-frequency peak. Each measuring point only contained the first-order low-frequency component, and the vibration amplitude decreased with the decrease of elevation. In order to verify the rationality and accuracy of this method for noise reduction of arch dam discharge structures, the measuring points B2, B3, B4, and B8 are analyzed, respectively.

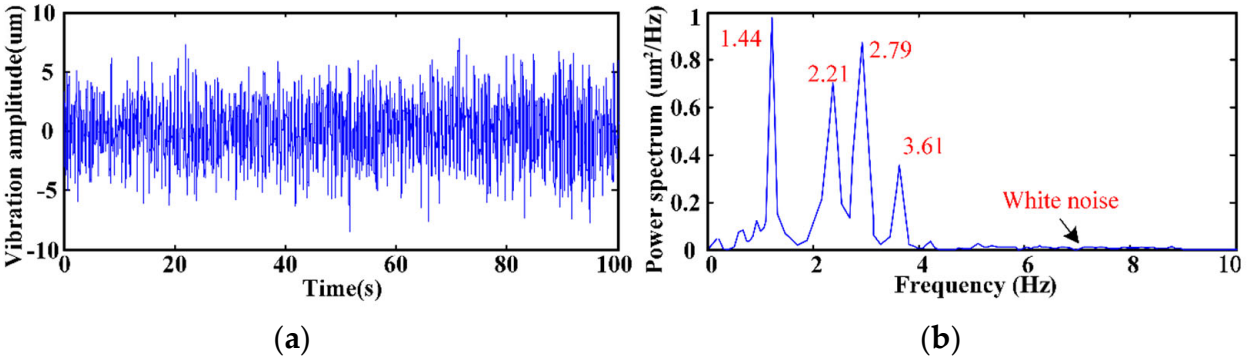

Figure 4. Time history signals and power spectra of B2 measuring point under condition 2. (**a**) Time history signals; (**b**) Normalized power spectra.

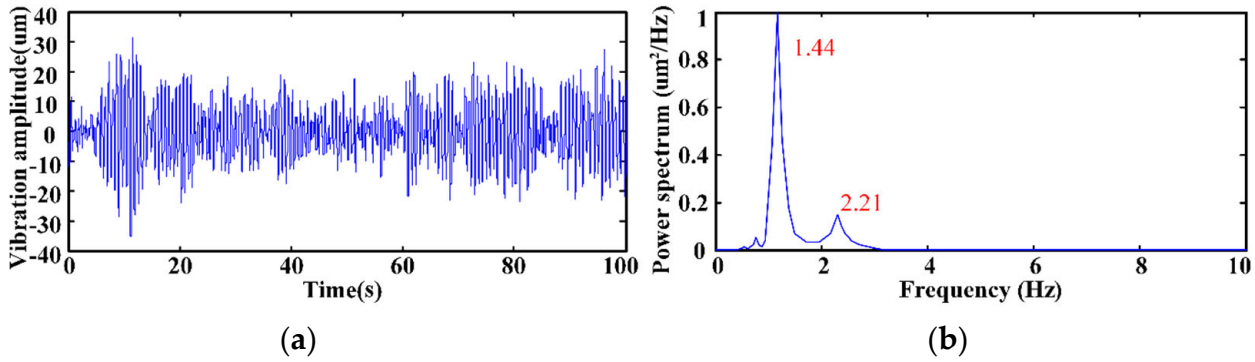

Figure 5. Time history signals and power spectra of B3 measuring point under condition 2. (**a**) Time history signals; (**b**) Normalized power spectra.

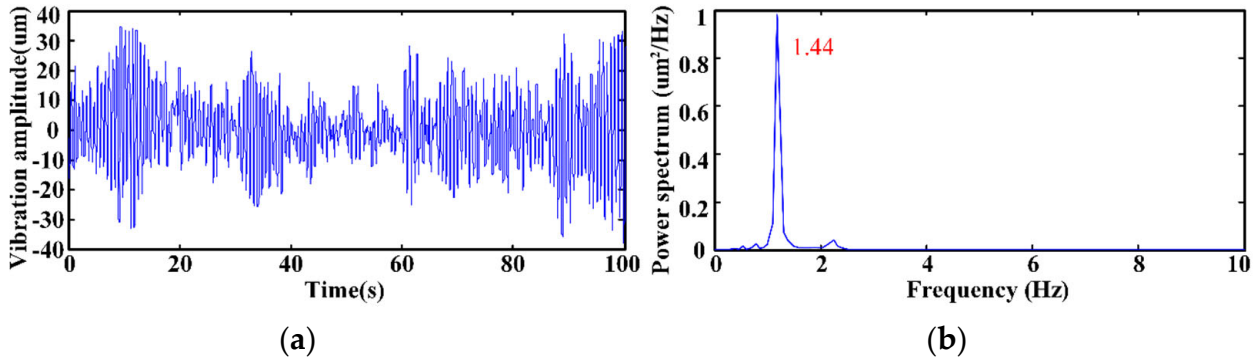

Figure 6. Time history signals and power spectra of B4 measuring point under condition 2. (**a**) Time history signals; (**b**) Normalized power spectra.

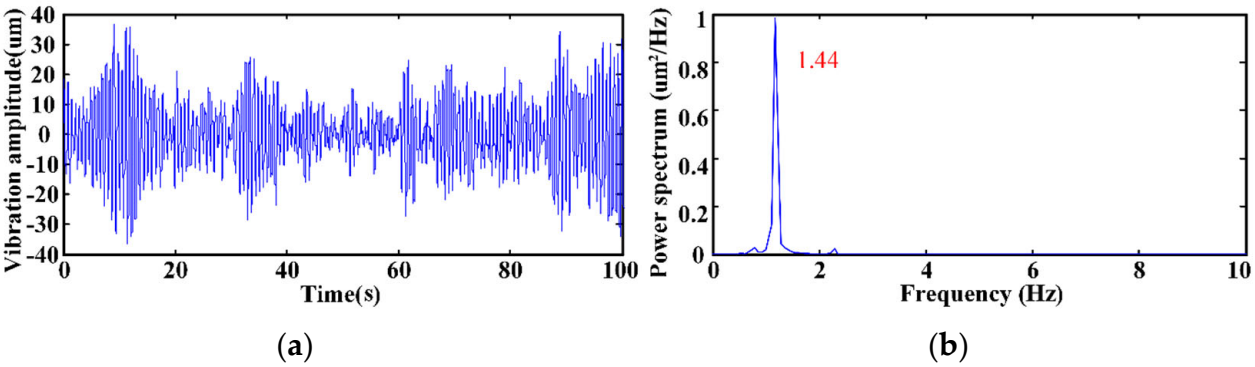

Figure 7. Time history signals and power spectra of B8 measuring point under condition 2. (**a**) Time history signals; (**b**) Normalized power spectra.

3.2. Improved Wavelet Threshold–EMD Hybrid Algorithm for Signal Noise Reduction

The original noise-containing signal and its normalized power spectral density curve are obtained, as shown in the Figure 3, on the basis of the measured displacement signal data of typical measurement point B2 under condition 2 of the arch dam. The time history diagram of the original signal and the power spectral density curve show that a large amount of white noise and low-frequency interference terms are mixed. The improved wavelet threshold–EMD hybrid algorithm was used to denoise the original signal. The time history diagram and the normalized power spectral density curve after filtering noise are shown in Figure 8.

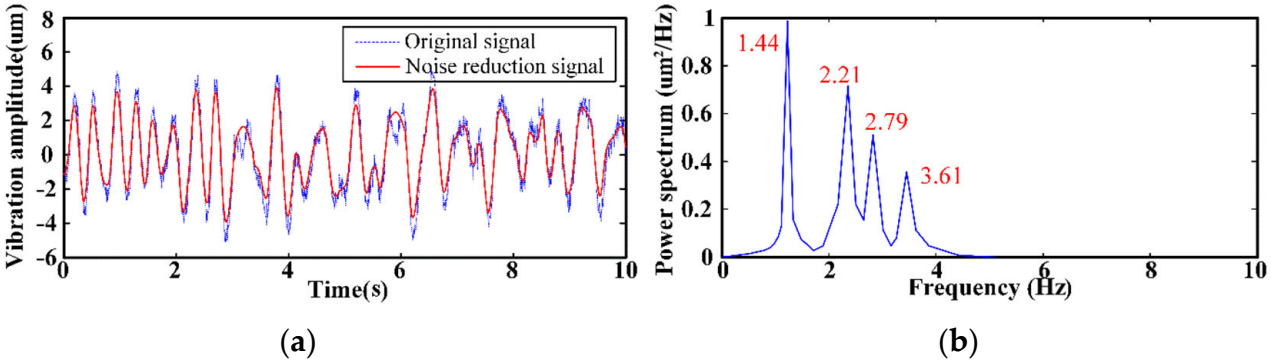

Figure 8. Time history diagram and the normalized power spectrum diagram after noise reduction. (**a**) Time history signals; (**b**) Normalized power spectra.

A comparison of the dam time history diagram before and after filtering is shown in Figure 4; it can be seen that many burrs appear in the original dam time history diagram of the arch dam. After filtering by this method, the burrs of the new time history diagram were eliminated. In the original power spectrum, many interference signals such as low-frequency interference signals and white noise were found. In the filtered new power spectrum, low-frequency interference signals below 0.5 Hz have been eliminated, and white noise has also been removed.

In further verifying the effectiveness and superiority of the noise reduction method, wavelet threshold denoising, EMD denoising, and the improved wavelet–EMD hybrid algorithm are used to process the vibration response signal of the arch dam. The results are shown in Figure 9.

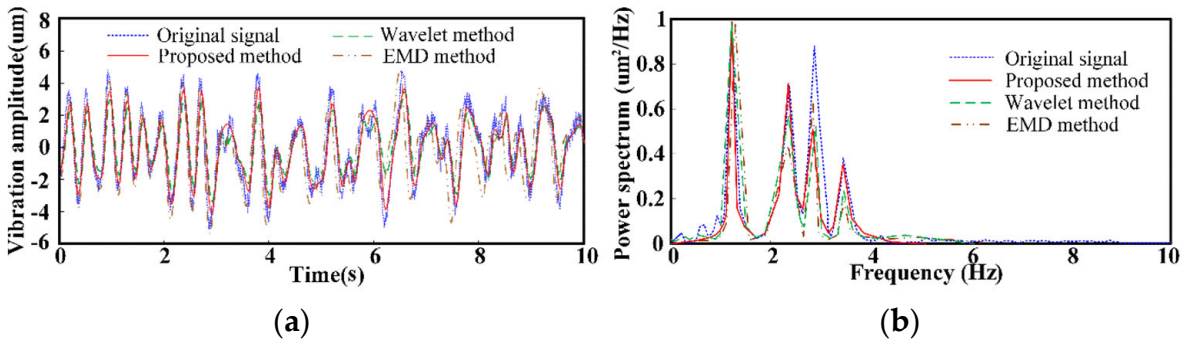

Figure 9. Comparison of calculation results of three noise reduction methods. (**a**) Time history signals; (**b**) Normalized power spectra.

Figure 8 shows that the improved wavelet threshold–EMD hybrid algorithm works better than the two other methods of noise reduction. Wavelet threshold denoising can remove high-frequency noise but cannot remove low-frequency flow noise. As a result, the signal is subject to large losses, and no excellent filtering effect is achieved. The EMD method effectively removes the low-frequency water flow noise during filtering but causes modal aliasing easily, which results in difficulty in the modal identification of high arch dam structures. The improved wavelet threshold–EMD hybrid algorithm is used in the study: the wavelet threshold filters the high-frequency noise signal, inhibits the EMD endpoint effect, and reduces the modal aliasing. Then, EMD decomposition is used to further filter low-frequency flow noise and white noise. This method retains the useful signal components as much as possible and reflects the effective feature information of the structure. Therefore, the improved wavelet threshold–EMD hybrid algorithm is suitable for the noise reduction of the vibration signals of high arch dam discharge structures.

3.3. Modal Identification of Working Parameters of High Arch Dam Discharge Structures

After the measured vibration response is filtered, the combination of HHT and RDT is used to identify the working modal of the high arch dam discharge structure under discharge excitation. The power spectral density curve in Figure 4 has peaks in many places. Considering the absence of mode aliasing, the pass band is taken directly by band-pass filtering, and the pass bands are 1–1.5 Hz, 1.5–2 Hz, 2– 2.5 Hz, 2.5–3 Hz, 3–4 Hz, 4–5 Hz, 5–6 Hz, 6–8 Hz, and 8–10 Hz, respectively. After filtering, 10 components of Y_1–Y_{10} are obtained. The power spectrum of these components is shown in Figure 10.

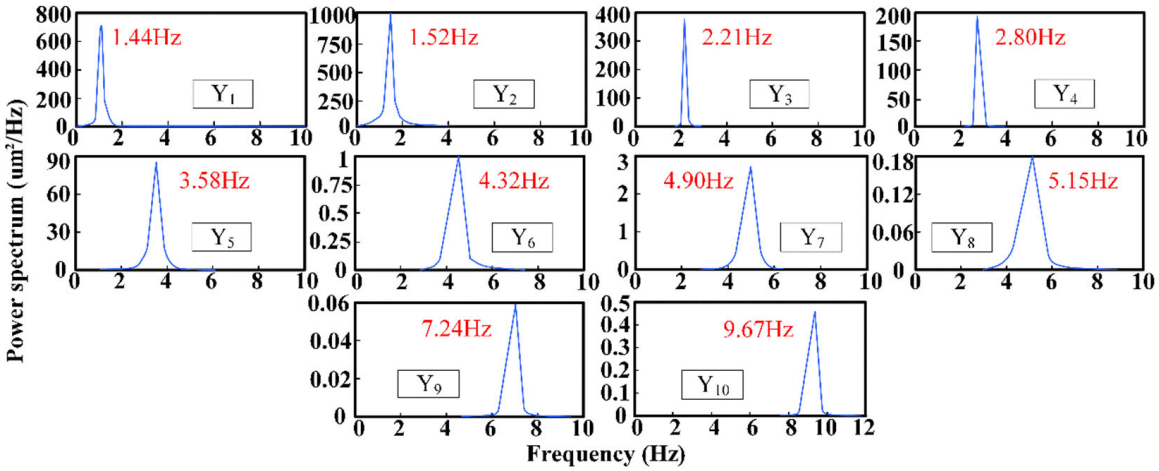

Figure 10. Power spectral of Y_1~Y_{10} components.

The free attenuation response of each component is extracted by RDT, the HHT and least squares fitting are used to obtain the relationship between amplitude and phase with time, and then the natural frequency and damping ratio of the structure are obtained. The time history diagram and power spectral of Y_1 are shown in Figure 11a,b. The logarithmic amplitude curves of the free-decay response signal and the least squares fit are shown in Figure 11c,d.

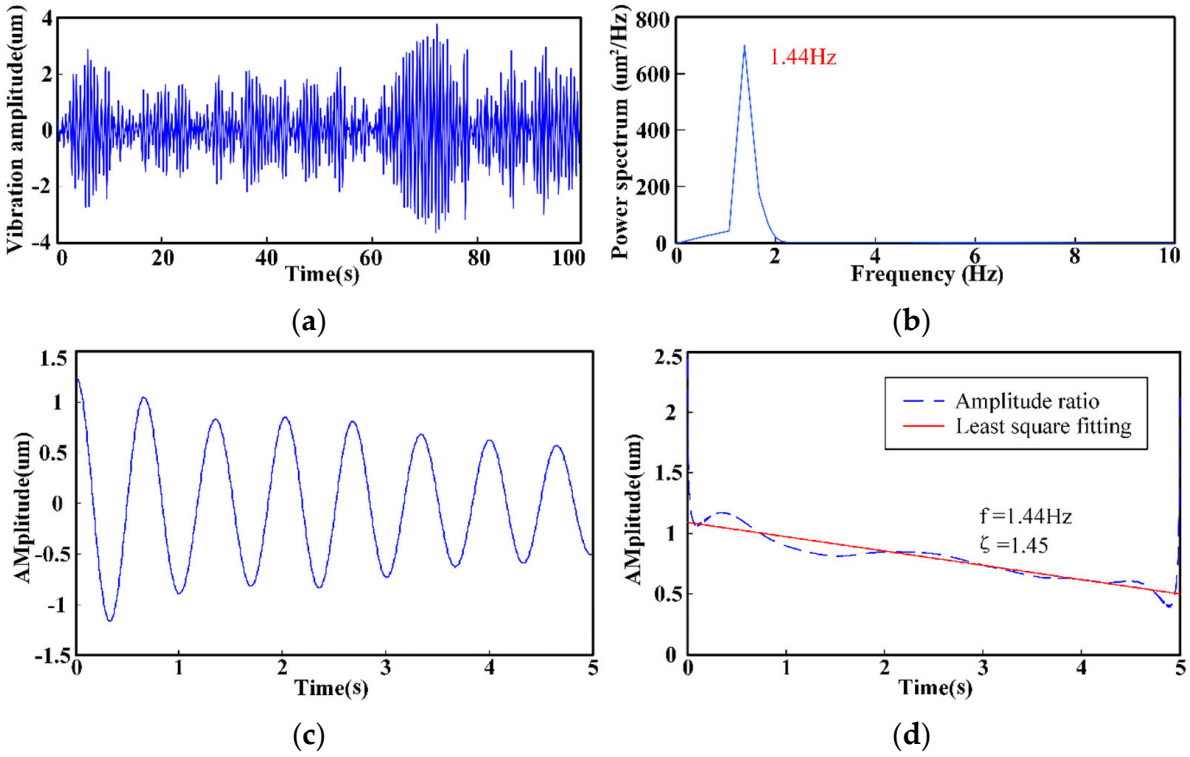

Figure 11. Process of modal parameters identification of Y1 component. (**a**) Time history; (**b**) Power spectra; (**c**) Free attenuation response; (**d**) Logarithmic amplitude curve.

The natural frequency and damping ratio of the first 10 orders of measurement points from B2, B3, B4, and B8 were obtained in sequence using the aforementioned method, and the recognition results are shown in Table 2. The recognition results show that the method in application can identify the natural frequency and damping ratio of the first 10 orders of the arch dam.

Table 2. Comparison of modal identification results of different measuring points of the high arch dam structure.

Modal / Order	Natural Frequency/Hz				Damping Ratio/%			
	B2	B3	B4	B8	B2	B3	B4	B8
1	1.44	1.44	1.44	1.43	1.45	1.79	1.51	1.69 1.91
2	1.52	1.53	1.52	1.53	1.54	1.08	1.26	1.35
3	2.21	2.19	2.19	2.20	1.45	1.28	2.24	1.46
4	2.80	2.81	2.78	2.81	1.48	1.46	2.17	1.28
5	3.58	3.60	3.59	3.61	1.31	3.47	4.08	1.79
6	4.32	4.31	4.32	4.28	4.38	4.96	6.5	5.6
7	4.90	4.90	4.92	4.91	2.18	1.93	3.67	2.38
8	5.15	5.12	5.20	5.21	2.86	5.5	2.87	6.72
9	7.24	7.28	7.30	7.26	7.67	7.16	8.12	7.47
10	9.67	9.69	9.58	9.52	4.79	6.45	6.45	5.34

The recognition results indicate that the identification working frequencies of each order of each measuring point are very close, the frequency identification error is within 3%, and the damping ratio of each order is within 9%. To further explain the rationality of the modal identification results of the high arch dam, the modal parameters were calculated by the eigensystem realization algorithm (ERA) method [40], ARX [41] method and Ibrahim time domain (ITD) method [42]. The results for natural frequency are shown in Table 3.

Table 3. Modal frequency identification of the high arch dam discharge structure with different methods.

Modal Order	Method in the Study/Hz	ERA/Hz	ARX/Hz	ITD/Hz
1	1.44	1.45	1.42	1.43
2	1.52	1.53	1.47	1.51
3	2.21	2.22	2.14	2.08
4	2.80	2.87	2.81	2.79
5	3.58	3.74	3.68	3.63
6	4.32	4.38	4.40	4.32
7	4.9	4.82	4.71	4.85
8	5.15	5.09	5.03	/
9	7.24	7.36	6.98	7.01
10	9.67	9.52	9.16	/

Table 3 shows that the results obtained using the proposed method are more consistent than those obtained by other typical identification methods. The proposed method can accurately determine the natural frequency and damping ratio of the structure and can identify its higher modal order. ERA can accurately identify the first six natural frequencies of the structure; however, as the order increases, the ERA method cannot fully identify the frequency of the structure because of the difficulty in order determination, thereby affecting the work mode recognition results of the structure. The order of the ARX method is difficult to determine; thus, frequency mixing in the structure easily occurs, and distinguishing the characteristic frequency is difficult. These factors bring difficulties to the recognition. The ITD method can identify the frequency information accurately but cannot fit the higher-order modes. The proposed improved wavelet threshold–EMD and RDT algorithm involves two processes. The first process uses the improved wavelet threshold–EMD method to reduce noises of the original signal, retain the main characteristic information, and reduce the influence of modal aliasing. The second process applies the improved RDT algorithm to the working modal parameter identification of the high arch dam discharge structure. The band-pass filter is used to control the EMD process of the vibration response signal to obtain the modal components of the structure, the RDT method is used to extract the free attenuation information of each modal component, and the natural frequency and damping ratio of the first 10 orders of the structure are identified. This method avoids complex system ordering and frequency mixing in modal decomposition. The principle is simple and solving large matrices is not required during calculation. Therefore, the proposed method can be used for modal parameter identification under the discharge excitation response of high arch dams and can be applied to other engineering applications.

4. Conclusions

An improved modal threshold identification method for high arch dam discharge structures is proposed. This method can eliminate the high-frequency white noise and reduce the influence of the modal aliasing effectively and identify the modal parameters of high arch dam discharge structures accurately. The specific conclusions are as follows:

1. An improved wavelet threshold–EMD hybrid algorithm is proposed for noise reduction pretreatment on measured vibration response data of high arch dams. The improved wavelet threshold algorithm was adapted to overcome the defect of soft and hard threshold function selection, which can effectively eliminate the high-frequency white noise and reduce the influence of the modal aliasing. Then, EMD further

eliminates the low-frequency flow noise and white noise, improving the accuracy of filtering and noise reduction.

2. An improved wavelet threshold–EMD and RDT algorithm is proposed for working mode identification of high arch dam discharge structures under the working environment load excitation. The proposed method avoids the complicated system ordering process and accurately identifies the modal parameters of high arch dam discharge structures. This method has a simple principle and does not require solving large matrices during calculation. The result has strong robustness and high identification accuracy.
3. The engineering examples show that the proposed method can accurately extract the work characteristic information of structures, has good noise reduction capabilities, and has high recognition accuracy. Therefore, this method eases the working modal parameter identification of high arch dam discharge structures and can be used for working modal recognition of other large frequency-intensive structures.

Author Contributions: Conceptualization, funding, B.W.; methodology, validation, formal analysis, resources, data curation, writing—original draft preparation, Y.G. and Z.Y.; visualization supervision, project administration, Y.G. and B.W. All authors have read and agreed to the published version of the manuscript.

Funding: This work was partially supported by the National Natural Science Foundation of China (grant numbers 52169025, 51779115, 51869011), Science and Technology Project of the Jiangxi Provincial Department of Water Resources (grant numbers: 202224ZDKT21,202223YBKT43), Jiangxi Provincial Department of Education, with focus on science and technology projects (grant number: GJJ206001).

Institutional Review Board Statement: The study did not require ethical approval.

Informed Consent Statement: The study did not involve humans.

Data Availability Statement: Not applicable.

Conflicts of Interest: The authors declare no conflict of interest.

References

1. Li, H.; Wang, Y.; Wei, B. Inversion algorithm for the whole prototype dynamic displacement field of a high arch dam based on limited measuring points. *J. Vib. Control.* **2017**, *23*, 3431–3447. [CrossRef]
2. Chengye, L.; Wei, L.; Bin, M.; Mingfu Song. Research on modal parameter identification method of high arch dam based on improved HHT. *J. Hydroelectr. Eng.* **2012**, *31*, 48–55.
3. Cheng, L.; Tong, F. Application of Blind Source Separation Algorithms and Ambient Vibration Testing to the Health Monitoring of Concrete Dams. *Math. Probl. Eng.* **2016**, *4*, 1–15. [CrossRef]
4. Bao, Y.; Xia, H.; Bao, Z.; Ke, S.; Li, Y. Structural Damage Identification of Pipe Based on GA and SCE-UA Algorithm. *Math. Probl. Eng.* **2013**, *2013*, 9. [CrossRef]
5. Li, H.; Wang, G.; Wei, B.; Zhong, Y.; Zhan, L. Dynamic inversion method for the material parameters of a high arch dam and its foundation. *Appl. Math. Model.* **2019**, *71*, 60–76. [CrossRef]
6. Wei, B.; Xie, B.; Li, H.; Zhong, Z.; You, Y. An improved Hilbert–Huang transform method for modal parameter identification of a high arch dam. *Appl. Math. Model.* **2021**, *91*, 297–310. [CrossRef]
7. Menghui, X.; Nan, J. Dynamic load identification for interval structures under a presupposition of 'being included prior to being measured. *Appl. Math. Model.* **2020**, *85*, 107–123.
8. Wei, P.; Li, Q.; Sun, M.; Huang, J. Modal identification of high-rise buildings by combined scheme of improved empirical wavelet transform and Hilbert transform techniques. *J. Build. Eng.* **2022**, *63*, 105443. [CrossRef]
9. Shangqing, Z.; Jiuzhang, L. Modal Test Analysis of Tied Arch Bridge Based on Random Subspace Method. *Munic. Technol.* **2015**, *33*, 38–41.
10. Loh, C.H.; Wu, T.C. System identification of Fei-Tsui arch dam from forced vibration and seismic response data. *J. Earthq. Eng.* **2000**, *4*, 511–537. [CrossRef]
11. Xueyuan, N.; Hua, D. Discussion on Modal Parameter Identification Method Based on Random Decreasing Technology. *Mech. Des.* **2012**, *29*, 1–5.
12. Chun, R.; Cheng Cheng, Z.; Qi Feng, L. Application of HHT Method in Time Domain Identification of Structural Modal Parameters. *J. Yangtze Univ.* **2008**, *5*, 115–118, 414.
13. Feldman, M. Time-varying vibration decomposition and analysis based on the Hilbert transform. *J. Sound Vib.* **2005**, *295*, 518–530. [CrossRef]

14. Huokun, L.; Jijian, L. Opperational Modal Parameter Identification of High Arch Dam Under flood discharge exciting Based on Frequency Domain Decomposition Method. *J. Vib. Shock.* **2008**, *27*, 149–153.
15. Li, H.; Liu, B.; Huang, W.; Liu, H.; Wang, G. Vibration load identification in the time-domain of high arch dam under discharge excitation based on hybrid LSQR algorithm. *Mechanic* **2020**, *177*, 109193. [CrossRef]
16. Pengming, T.; Junyi, L.; Feng, Z. Application of Random Decrement Method in Identification of Working Modal Parameters. *Mech. Electr. Eng. Technol.* **2012**, *41*, 105–108.
17. Wenge, T.; Xiaobing, Z. Working Mode Recognition Based on HVD and RDT. *J. Guangxi Univ.* **2018**, *43*, 132–140.
18. Jianwei, Z.; Lianghuan, Z.; Qi, J.; Yu, Z.; Jia, G. Identification of working modal parameters of high dam discharge structure based on HHT. *Vib. Meas. Diagn.* **2015**, *35*, 777–783, 804.
19. He, X.H.; Hua, X.G.; Chen, Z.Q.; Huang, F.L. EMD-based random decrement technique for modal parameter identification of an existing railway bridge. *Eng. Struct.* **2011**, *33*, 1348–1356. [CrossRef]
20. Frank Pai, P.; Palazotto, A.N. HHT-based nonlinear signal processing method for parametric and non-parametric identification of dynamical systems. *Int. J. Mech. Sci.* **2008**, *50*, 1619–1635. [CrossRef]
21. Jianping, H.; Lin, L.; Hongtao, W.; Wei, Q. Modal parameter identification based on Hilbert-Huang transform and random decrement technique. *World Earthq. Eng.* **2011**, *27*, 72–77.
22. Jinyuan, T.; Weitao, C.; Siyu, C.; Wei, Z. A new wavelet threshold function and its application in vibration signal denoising analysis. *J. Vib. Shock.* **2009**, *28*, 118–121.
23. Zhisong, L. Signal Denoising Method Based on Wavelet Analysis. *J. Zhejiang Ocean. Univ.* **2011**, *30*, 150–154.
24. Xiuping, L.; Wei, Y.; Lili, H.; Junfeng, J.; Jian, X.; Zebin, S.; Haifeng, S. X-ray pulsar signal de-noising for impulse noise using wavelet packet. *Aerosp. Sci. Technol.* **2017**, *64*, 147–153. [CrossRef]
25. Wenwen, Z.; Xingwen, C. A New EMD Denoising Method. *Electron. Technol.* **2008**, *21*, 30–32, 36.
26. Dybała, J.; Zimroz, R. Rolling bearing diagnosing method based on Empirical Mode Decomposition of machine vibration signal. *Appl. Acoust.* **2014**, *77*, 195–203. [CrossRef]
27. Chengye, L.; Jijian, L.; Wei, L.; Bin, M. Improvement of Joint Filtering Method of EMD and Wavelet Threshold and Its Application in Vibration Analysis of Discharge Structure. *J. Vib. Shock.* **2013**, *32*, 63–70, 110.
28. Jintao, Y.; Shuyan, Z.; Wei, W. Denoising of Transmitted Signal Based on Empirical Mode Decomposition and Wavelet Transform. *J. Harbin Inst. Technol.* **2011**, *43*, 88–92.
29. Aijun, H.; Jingjing, S.; Ling, X. Modal aliasing problem in empirical mode decomposition. *Vib. Test. Diagn.* **2011**, *43*, 429–434.
30. Jianwei, Z.; Qi, J.; Yu, Z.; Lianghuan, Z.; Jia, G. A Signal Denoising Method Suitable for Vibration Analysis of Discharge Structures. *J. Vib. Shock.* **2015**, *34*, 179–184.
31. Zhi, C.; Feng, H.; Xiaolong, Z.; Xu, J.; Zailong, H. Wavelet-experience mode decomposition method for trend term modulation for atmospheric dry length profile denoising. *Acta Opt. Sin.* **2017**, *37*, 15–26.
32. Wei, B.W.; Yuan, D.Y.; Li, H.K.; Xu, Z. Combination forecast model for concrete dam displacement considering residual correction. *Struct. Health Monit.* **2017**, *18*, 232–244. [CrossRef]
33. Wei, B.W.; Yuan, D.Y.; Li, H.K.; Li, L. Modified hybrid forecast model considering cjhaotic residual errors for dam deformation. *Struct. Control. Health Monitor.* **2018**, *25*, e2188. [CrossRef]
34. Wei, L.; Xiaohui, C.; Haijie, M. Research on adaptive determination of decomposition layer in wavelet threshold denoising algorithm. *Comput. Simul.* **2009**, *26*, 311–313, 336.
35. Yang, J.; Lia, P.; You, Y.; Dian, X. An improved EMD method for modal identification and a combined static-dynamic method for damage detection. *J. Sound Vib.* **2018**, *28*, 242–260. [CrossRef]
36. Qinwei, R.; Wei, L.; Ce, S.; Hongzhi, K. Research on EMD dense modal identification and its application in power plant buildings. *J. Hydroelectr. Eng.* **2017**, *36*, 103–113.
37. Mert, A.; Akan, A. Detrended fluctuation thresholding for empirical mode decomposition based denoising. *Digit. Signal Proc.* **2014**, *32*, 48–56. [CrossRef]
38. Wenping, H.; Qiong, W.; Haiying, C.; Wen, Z. Comparison of different filtering methods for denoising in detrended wave analysis. *Acta Phys. Sin.* **2011**, *60*, 029203.
39. Fubin, L.; Xiangming, G. Hurst Exponent Estimation Based on EEMD and DFA. *Meas. Control. Technol.* **2013**, *32*, 98–101.
40. Jijian, L.; Hunkun, L.; Jianwei, Z. Hydraulic structure vibration mode ERA recognition method based on singular entropy fixed-stage noise reduction. *Chin. Sci.* **2008**, *38*, 1398–1413.
41. Wen, Y.; Guoming, L.; Wei, L. Modal analysis of nozzle concrete gravity dam based on strong earthquake record. *Earthq. Eng. Eng. Vib.* **2014**, *34*, 25–33.
42. Shengkui, D.; Deqiang, Z.; Jian, L. Structural modal parameter identification based on ITD method. *J. Civ. Eng. Manag.* **2012**, *29*, 15–19.